JAIST Repository
https://dspace.jaist.ac.jp/

Title	Modeling of High-Speed, Large-Signal Transistor Switching Transients from s-Parameter Measurements
Author(s)	Ikawa, Yasuo; Eisenstadt, William R.; Dutton, Robert W.
Citation	IEEE Transactions on Electron Devices, 29(4): 669-675
Issue Date	1982-04
Type	Journal Article
Text version	publisher
URL	http://hdl.handle.net/10119/5004
Rights	Copyright (C)1982 IEEE. Reprinted from IEEE Transactions on Electron Devices, 29(4), 1982, 669-675. This material is posted here with permission of the IEEE. Such permission of the IEEE does not in any way imply IEEE endorsement of any of JAIST's products or services. Internal or personal use of this material is permitted. However, permission to reprint/republish this material for advertising or promotional purposes or for creating new collective works for resale or redistribution must be obtained from the IEEE by writing to pubs-permissions@ieee.org. By choosing to view this document, you agree to all provisions of the copyright laws protecting it.
Description	

JAIST
JAPAN ADVANCED INSTITUTE OF SCIENCE AND TECHNOLOGY

Japan Advanced Institute of Science and Technology

Modeling of High-Speed, Large-Signal Transistor Switching Transients from s-Parameter Measurements

YASUO IKAWA, MEMBER, IEEE, WILLIAM R. EISENSTADT, STUDENT MEMBER, IEEE, AND ROBERT W. DUTTON, SENIOR MEMBER, IEEE

Abstract—**A new technique has been developed to derive the large-signal transient response of semiconductor devices from small-signal frequency response data. The large-signal switching response can be calculated for an arbitrary input signal voltage and rise time. This new technique utilizes the Fourier transformation to combine arrays of small-signal data to compute the response waveform.**

The input waveform is decomposed into a superposition of small pulses. The response to each pulse is obtained by Fourier transformation techniques, using s-parameter data at appropriate bias points. The sum of these responses approximates the overall transient response. Simulations were performed for a GaAs MESFET for step inputs with the rise times of 8 ns and 150 ps. Good agreement was obtained between simulated waveforms and measured output waveforms in rise time, magnitude, and waveform shape.

This algorithm is general and will work for other measured small-signal transfer parameters as functions of frequency and bias.

INTRODUCTION

TWO METHODS dominate the measurement of semiconductor device high-speed characteristics. Frequency-domain measurements such as s-parameters display complex, small-signal information. Time-domain measurements capture large-signal switching rise times, magnitudes, and waveforms. s-parameter measurements are generally employed for bipolar transistor and GaAs FET measurements in contrast to time-domain techniques which are utilized in FET switching and ring oscillator measurements. For passive linear circuit elements, the two measurement techniques yield the same information. This information can be converted from time domain to frequency domain and back through the Fourier transformation and inverse transformation.

On the other hand, the reconciliation of active device information in the time and frequency domain poses a difficult and unsolved problem. A novel technique is presented which models active semiconductor device large-signal switching characteristics in the time domain using s-parameter data.

The major difficulty in reconciling the small-signal and switching transient characterization techniques for active devices is the fact that the s-parameter transfer response is bias dependent. As a device switches, it crosses a continuum of separate bias conditions with corresponding s-parameter frequency data. In order to produce a tractable analytical solution based on s-parameter data, device operation in quasi-static mode must be assumed. This assumption is shown to be valid for GaAs MESFET's studied.

Manuscript received October 5, 1981; revised December 21, 1981. This work was supported in part by the Army Research Office under Contract DAAG29-80-K-0013, as well as by Hewlett-Packard and Tektronix under industrial grants.

Y. Ikawa is with the Integrated Circuits Laboratory, Stanford University, Stanford, CA 94305, on leave from Toshiba Research and Development Center, Kawasaki, Japan.

W. R. Eisenstadt and R. W. Dutton are with the Integrated Circuits Laboratory, Stanford University, Stanford, CA 94305.

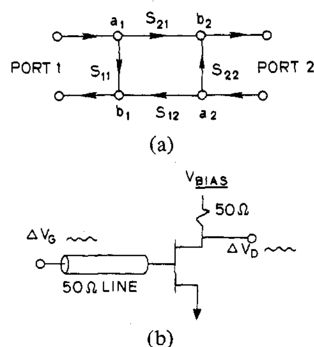

Fig. 1. s-parameter flow diagram and conceptual representation of FET s-parameter measurement.

The approximation technique which has been developed derives the large-signal transient response of semiconductor devices from s-parameters using multiple Fourier transformations. The algorithm employed is designed to be efficient and readily implementable on a fast desktop calculator or minicomputer.

s-PARAMETER MEASUREMENTS OF SEMICONDUCTOR DEVICES

At very high frequencies, s-parameters may be the only practical characterization method available. Moreover, s-parameter data can be readily transformed into y-, h-, and z-parameters. In the technique discussed here, the output response of a device to an input pulse of arbitrary rise time and magnitude is modeled using s_{21}. Fig. 1 illustrates the flow diagram and physical configuration for the measurement of s_{21} of a FET.

In the flow diagram, a_n is the complex incident signal voltage at port n, and b_n is the complex reflected signal voltage at port n:

$$s_{21} = \frac{b_2}{a_1}\bigg|_{a_2=0} = \frac{\Delta V_D}{\Delta V_G}. \tag{1}$$

s_{21} is the output at port 2 divided by the input at port 1 when there is no incident signal at port 2. For the FET, this is

0018-9383/82/0400-0669$00.75 © 1982 IEEE

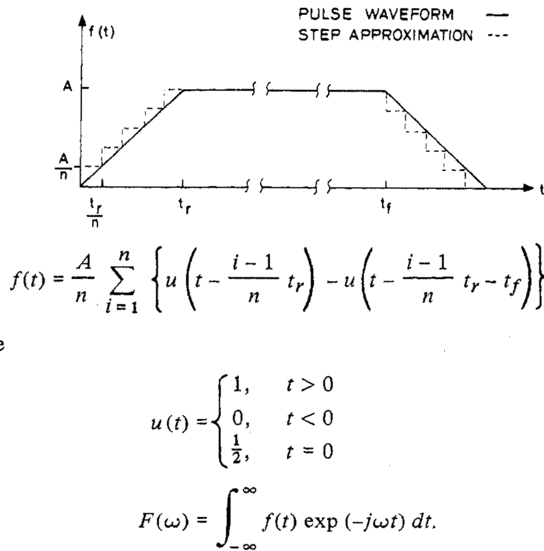

$$f(t) = \frac{A}{n} \sum_{i=1}^{n} \left\{ u\left(t - \frac{i-1}{n} t_r\right) - u\left(t - \frac{i-1}{n} t_r - t_f\right) \right\}$$

where

$$u(t) = \begin{cases} 1, & t > 0 \\ 0, & t < 0 \\ \frac{1}{2}, & t = 0 \end{cases}$$

$$F(\omega) = \int_{-\infty}^{\infty} f(t) \exp(-j\omega t)\, dt.$$

Fig. 2. Approximation of input pulse waveform.

equivalent to the drain output signal divided by the gate input signal. Both incident and reflected signals depend on the system impedance, which means s_{21} is dependent on the system impedance. In this work, measurements were performed with the common system impedance of 50 Ω for both input and output.

Details of the Modeling Technique

In this section, the detailed modeling technique is described which simulates time-domain waveforms in the nonlinear region of transistors using s-parameter small-signal data. The input pulse waveform is approximated as shown in Fig. 2, that is, the input waveform is decomposed into n small pulses—each with a different delay time. In order to express the mathematical algorithm, let $f'(t)$ be a simplified pulse function: $f'(t) = u(t) - u(t - t_f)$, a pulse with width t_f. Using the time-delayed forms of $f'(t)$, the large pulse waveform in Fig. 2 can be expressed as

$$f(t) = \sum_{i=1}^{n} \frac{A}{n} f'\left(t - \frac{i-1}{n} t_r\right) \tag{2}$$

where t_r is the total rise time and n is the number of discretized steps. The ith delayed pulse $f'^{(i)} = f'(t - ((i-1)/n)\, t_r)$ is Fourier transformed into the frequency domain to yield $F'^{(i)}(\omega)$, which is given by

$$F'^{(i)}(\omega) = F'(\omega) \exp\left(-j\omega \frac{i-1}{n} t_r\right) \tag{3}$$

where

$$F'(\omega) = \frac{1 - \exp(-j\omega t_f)}{j\omega} = t_f \operatorname{sinc}\left(\frac{\omega t_f}{2}\right) \exp\left(\frac{-j\omega t_f}{2}\right). \tag{4}$$

This $F'^{(i)}(\omega)$ is multiplied by $s_{21}^{(i)}(\omega)$, which is the measured s_{21} data at the corresponding bias level, giving the output function $G'^{(i)}(\omega) = F'^{(i)}(\omega)\, s_{21}^{(i)}(\omega)$. To illustrate the meaning of this multiplication, $F'^{(1)}(\omega) = F'(\omega)$ and $s_{21}^{(1)}(\omega) = s_{21}(\omega)$ are schematically shown in Fig. 3. After the multiplication in the frequency domain, the output signal responding to this small delayed pulse $f'^{(i)}$ is calculated by the inverse Fourier transformation of $G'^{(i)}(\omega)$.

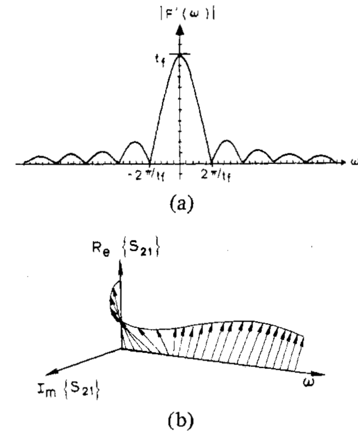

Fig. 3. Conceptual representation of simplified pulse function and s-parameter data to be multiplied in the frequency domain to obtain an output function. (a) $F'(\omega) = t_f \operatorname{sinc}(\omega t_f/2) \exp(-j(\omega t_f/2))$. (b) Complex s_{21} data.

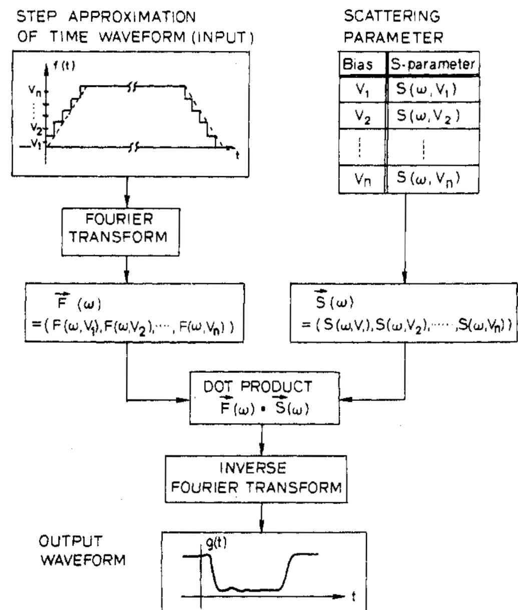

Fig. 4. Simulation procedure. An input switching pulse is segmented into voltage steps and Fourier transformed. The results are multiplied by s-parameters at appropriate voltages and summed. An inverse Fourier transformation yields the switching waveform.

In order to calculate the response to a large pulse $f(t)$ in Fig. 2, which is no longer considered to be small-signal and in the linear region, the approximation algorithm illustrated in Fig. 4 is employed. The Fourier transformation $(A/n)\, F'^{(i)}(\omega)$ of each delayed small-signal pulse becomes a component in a vector $\bar{F}(\omega)$. A second vector $\overline{S_{21}}(\omega)$ is created using $s_{21}^{(i)}(\omega)$ as each component. A vector dot product is then taken to form $G(\omega) = \bar{F}(\omega) \bullet \overline{S_{21}}(\omega)$, which is a linear superposition in

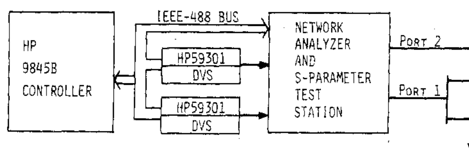

Fig. 5. s-parameter measurement system configuration.

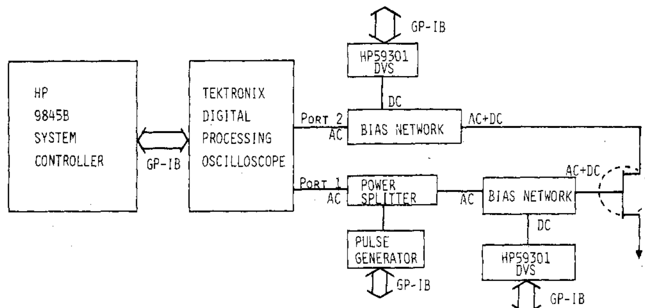

Fig. 6. Time-domain waveform measurement system configuration.

the frequency domain to obtain the output function of the nonlinear system.[1] This calculation assumes that the intrinsic pulse response of FET is fast enough to be considered as only bias dependent and not otherwise dependent on time over the region of simulation—thus the FET must be operated in the quasi-static mode.

In order to facilitate the calculation, $G(\omega)$ is split into two parts; a rising step and a delayed falling step, both modified by s_{21} data. Both steps have the same mathematical formula $G_0(\omega)$ except for the t_f-delay factor. The output waveform $g(t)$ can be expressed as $g(t) = g_0(t) - g_0(t - t_f)$ where $g_0(t)$ is the inverse Fourier transformation of $G_0(\omega)$.

Measurements for High-Speed Devices

Characteristics of GaAs MESFET's are measured using s_{21} obtained with the Stanford TECAP [1]-[3] automated measurement facility. The TECAP s-parameter software was modified to achieve enhancement of calibration and measurement accuracy and to adapt it to GaAs MESFET biasing capabilities.

The s-parameters are measured using a Hewlett-Packard (HP) 8505A network analyzer and an HP 8503A s-parameter test station. Fig. 5 shows the configuration of this measurement system. The system utilizes HP 9845B desktop computer, which provides measurement control through the IEEE-488 bus, as well as data storage and software for calibration. Bias voltages to the FET gate and drain are supplied by HP 6131C voltage sources through HP 59301 digital-to-analog converter controlled by the computer.

Time-domain measurements are performed on a newly developed subnanosecond time-domain measurement system, which is schematically shown in Fig. 6. A pulse generator or tunnel diode pulser supplies a pulse to the gate of a GaAs MESFET and to one channel of a Tektronix Digital Processing Oscilloscope (DPO). A dc offset can be added to the gate waveform through a bias network. The resultant drain switching waveform is separated into its ac and dc components by another bias network and the ac signal enters the other DPO channel. A voltage source is added to the dc input of a second bias network to provide a drain bias. The DPO contains a waveform digitizer and semiconductor memory which enables it to record and store four different waveforms. The system has the capability to measure rise times as short as 25 ps and to perform time-domain reflectometry [4], [5].

The desktop computer is utilized for the modeling technique calculation as well as measurement control and data acquisition. The simulation frequently requires hundreds of data points of s-parameter depending on the number of bias levels and frequency points. The amount of data has not been optimized with respect to modeling accuracy. An automated measurement and calculation system is the only practical method for the implementation of this modeling.

Implementation of Approximation Technique

A matrix of s_{21} data must be measured across a range of useful device bias conditions and the maximum frequency range of the network analyzer. The dc bias applied to the GaAs MESFET gate is varied from 0 to -2.5 V ($\approx$ pinchoff voltage) in 0.25-V steps. This range of dc biases traces a 50-Ω load line across the family of gate voltage curves on an I_D versus V_{DS} graph. At each 0.25 voltage level, the s_{21}-parameters are measured at 25 frequency points across the 0.5-MHz to 1.3-GHz range of the network analyzer. With this frequency range, the fastest input rise time which may be simulated is 0.27 ns.[2] For the simulation of the response to faster input, s_{21} data above 1.3 GHz were extrapolated from measured data.

As is described in the previous section and in Fig. 4, a step approximation of the input waveform is made and segmented into as many pulses as necessary both to accurately express the input waveform and to be consistent with the small-signal assumption in each segmented region. The Fourier transformation of each step is taken yielding a frequency band at each bias level. Frequency-domain information of the input signal forms a vector $\bar{F}(\omega) = (F_1(\omega), \cdots, F_n(\omega))$ and the s_{21} data obtained at appropriate bias points create a second vector $\overline{S_{21}}(\omega) = (s_{21}^{(1)}(\omega), \cdots, s_{21}^{(n)}(\omega))$. The dot product of these two vectors results in the output function $G(\omega)$ in the frequency domain—the inverse Fourier transformation yields the output waveform $g(t)$.[3]

The good agreement between the simulation based on s-parameter data and the measured switching response is displayed in Fig. 7. Here the calculated waveform is smooth while the measured waveform contains a small ac noise. The input waveform for this simulation is 8 ns in rise time and -2.5 V in magnitude. The simulated waveform displays a 4-ns rise time and 3.4-V swing while the measured waveform

[1] The vector dot product calculation is explained in Appendix I.

[2] The rise time T_r is related to the system 3-dB frequency f_B as shown in the following equation [6]: $f_B = 0.35/T_r$.

[3] The mathematical treatment for computer programming is presented in Appendix II.

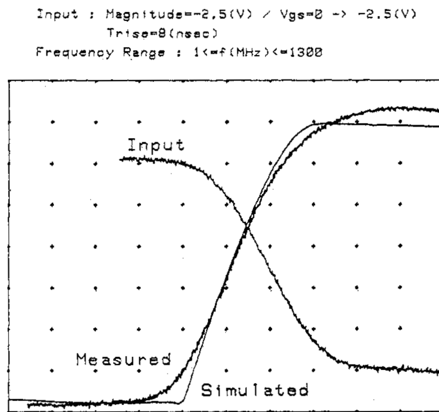

Fig. 7. Comparison of measured and simulated results of GaAs transistor switching for the input of 8-ns rise time. (Vert: 0.5 V/div, horiz: 2 ns/div.)

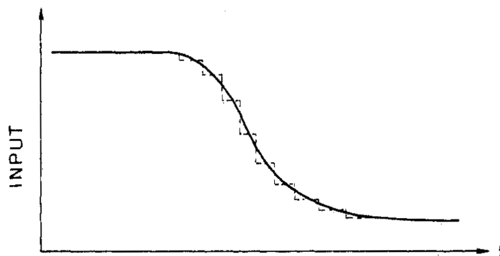

Fig. 8. The improved decomposition method for input pulse. The input pulse is decomposed into small pulses with arbitrary magnitude and delay.

displays a 5-ns rise time and 3.5-V change in magnitude. The waveform shapes are approximately the same. A major cause of error in this match is the approximation of the input waveform by an ideal ramp function—the actual input waveform increases more gradually at the start and end of the transition, resulting in a slower rise time.

In an effort to improve this approximation, a new method of decomposition of the input pulse into arbitrary sized small pulses was employed as shown in Fig. 8. In this method, the input pulse is expressed as the sum of small pulses with appropriate magnitude and delay time. Thus any input pulse waveshape can be correctly approximated. The comparison between the measured and the simulated output waveforms obtained by using the improved decomposition method is shown in Fig. 9 together with the measured input waveforms. This figure displays the output waveforms for large-signal input step magnitudes varied from -0.5 to -3.0 V. For these inputs, the waveshapes are identical and they are decomposed into the arbitrarily discretized 15 small pulses. This is in contrast to the equally discretized 22 small pulses in the case of Fig. 7. Agreement between the measured and simulated outputs is improved at the start and end of the transition as compared with Fig. 7. The slight deviation for the larger input magnitude is created by the roughness of decomposition.

The waveform in Fig. 10 presents a switching response of a GaAs MESFET for the input of 150 ps in rise time and 0.21 V in magnitude. This output waveform was simulated from only one input bias level of s_{21} data. The simulated waveform has a 170-ps rise time and a 0.5-V magnitude as opposed to the measured waveform with a 100-ps rise time, about 100-ps delay time, and a 0.45-V magnitude. The agreement between the modeled waveform and measured waveform is acceptable. A major cause of error with this simulation is the extrapolation of s_{21} data to frequencies higher than 1.3 GHz. Thus the s_{21} data do not exhibit correct components at the highest frequency in simulation of the time-domain waveforms. In spite of the capacity to simulate the delay time observed in the measured waveform, the waveform could not be modeled due to the lack of s-parameter data in the appropriate frequency range. This lack of s-parameter data and the finite bandwidth in the numerical calculation of inverse Fourier transformation cause the periodic oscillation before the occurrence of falling transition of the output. Taking the lack of higher frequency s-parameters into account, the agreement is very good for the waveforms of the time longer than 250 ps. This implies that a very accurate simulation can be carried out with proper higher frequency s-parameter data, since frequencies below 1.3 GHz are responsible for time-domain waveforms with rise time longer than 270 ps [6].

Discussion and Summary

The approximate modeling technique developed in this paper demonstrates good agreement between simulated and measured waveforms. The quasi-static approximation is applicable for GaAs MESFET's because these devices have intrinsic pulse response times on the order of tens of picoseconds [7], [8]. The modeling technique yields a reasonable result for FET switching behavior.

Many causes of error existed in this modeling exercise. The division of the input waveform into the finite number of pulse steps contributed to deviation in the simulation. The inability to measure s_{21} data above 1.3 GHz and the use of extrapolated data in this regime causes inaccuracy in the result for fast switching events. Limitations with time-domain measurement equipment, especially the bias network bandwidth, gives incorrect measurements for pulses longer than 20 ns.

On the other hand, despite many limitations for the highest frequency applications, the technique is extremely general. The measurements and modeling methods are applicable to FET's in general. s-parameters were employed because the highest frequencies available had to be measured in order to model GaAs. Other linear small-signal parameters that measure input-to-output gain can readily be substituted. Care must be taken to insure that the small-signal parameters are measured using the same impedances as the desired FET switching conditions to be simulated.

Appendix I
Vector Dot Product Calculation

In the linear system, time domain and frequency domain are related with each other through Fourier transform. Let the input and the output signal in the time and frequency domain be as follows:

	Time Domain	Frequency Domain
Input	$f(t)$	$F(\omega)$
Output	$g(t)$	$G(\omega)$

where

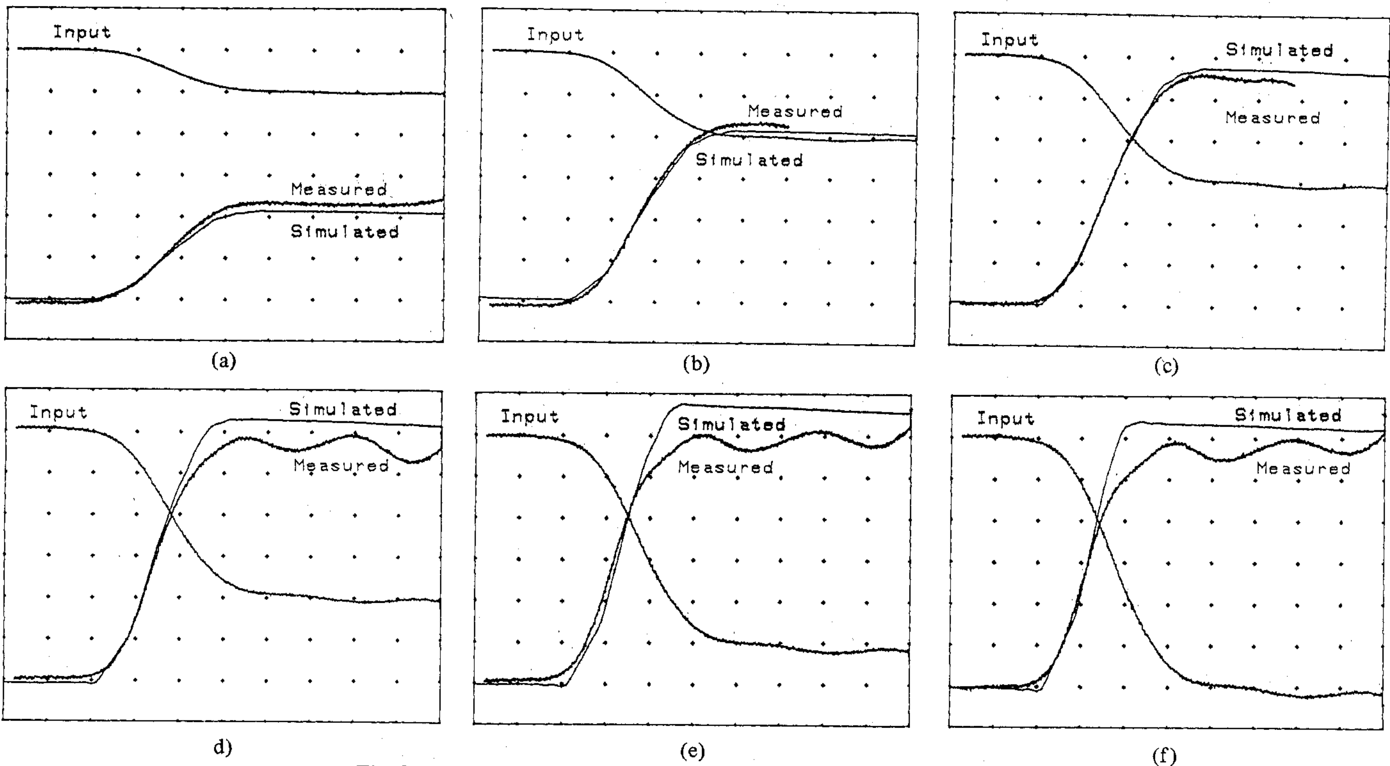

Fig. 9. Comparison between measured and simulated waveforms obtained by the improved input waveform approximation method. (Vert: 0.5 V/div, horiz: 2 ns/div.)

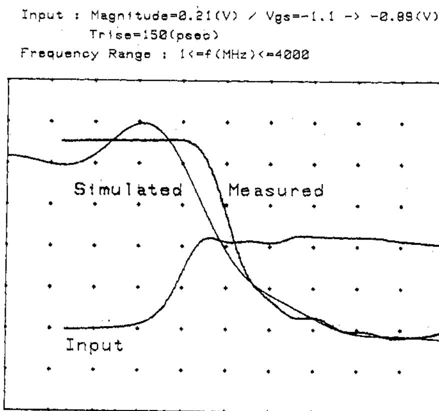

Fig. 10. Comparison of measured and simulated results of GaAs transistor switching for the input of 150-ps rise time. (Vert: 0.1 V/div, horiz: 100 ps/div.)

$$F(\omega) = \int_{-\infty}^{\infty} f(t) \exp(-j\omega t)\, dt$$

$$f(t) = \frac{1}{2\pi} \int_{-\infty}^{\infty} F(\omega) \exp(jt\omega)\, d\omega \tag{A1}$$

$$G(\omega) = \int_{-\infty}^{\infty} g(t) \exp(-j\omega t)\, dt$$

$$g(t) = \frac{1}{2\pi} \int_{-\infty}^{\infty} G(\omega) \exp(jt\omega)\, d\omega. \tag{A2}$$

An input-to-output transfer function is generally given in the frequency domain. s-parameter data are an example of this. Thus let a transfer function be given by $T(\omega)$. Then the output function $G(\omega)$ is given by

$$G(\omega) = F(\omega) \cdot T(\omega). \tag{A3}$$

Next consider an input signal in the time domain that is expressed by the addition of several signals.

$$f(t) = h_1(t) + h_2(t) + \cdots + h_n(t). \tag{A4}$$

A Fourier transform yields

$$F(\omega) = H_1(\omega) + H_2(\omega) + \cdots + H_n(\omega) \tag{A5}$$

where $H_i (i = 1, 2, \cdots, n)$ is the Fourier transform of $h_i(t)$. From (A3) and (A5)

$$G(\omega) = T(\omega) H_1(\omega) + T(\omega) H_2(\omega) + \cdots + T(\omega) H_n(\omega). \tag{A6}$$

This is true for the linear system.

Now (A6) will be extended to approximately represent a nonlinear system. In such a system, transfer function $T(\omega)$ is the superposition of the linear transfer functions.

$$T(\omega) = \begin{cases} T_1(\omega), & \text{if } f(t) = h_1(t) \\ T_2(\omega), & \text{if } f(t) = h_1(\infty) + h_2(t) \\ T_3(\omega), & \text{if } f(t) = h_1(\infty) + h_2(\infty) + h_3(t) \\ \cdots & \cdots \\ T_n(\omega), & \text{if } f(t) = h_1(\infty) + h_2(\infty) \\ & \quad + \cdots + h_{n-1}(\infty) + h_n(t). \end{cases} \tag{A7}$$

In order to combine (A6) and (A7), the following is assumed:

$$T(\omega) H_i(\omega) = T_i(\omega) H_i(\omega) \quad (i = 1, 2, \cdots, n). \tag{A8}$$

This means transfer function $T_i(\omega)$ operates on only the corresponding input signal $h_1(\infty) + h_2(\infty) + \cdots + h_{i-1}(\infty) + h_i(t)$. This is a necessary condition under nonlinear system to explain at least linear behavior. Using the assumption (A8), we obtain the output function $G(\omega)$ for the nonlinear system

$$G(\omega) = T_1(\omega) H_1(\omega) + T_2(\omega) H_2(\omega) + \cdots + T_n(\omega) H_n(\omega). \tag{A9}$$

In applying this relation to transistors, suppose $t_f = \infty$ and let $h_i(t)$ be a small step pulse $f'^{(i)}(t)$, and $T_i(\omega)$ be the s_{21}-parameter $s_{21}^{(i)}(\omega)$ for the identical bias condition. Thus we obtain

$$G(\omega) = \sum_{i=1}^{n} s_{21}^{(i)}(\omega) \cdot F'^{(i)}(\omega) = \overline{F}(\omega) \bullet \overline{S_{21}}(\omega) \tag{A10}$$

which is a vector dot product.

Appendix II
Mathematical Treatment for Computer Programming

In order to do the simulation, it is necessary to perform the numerical calculation of inverse Fourier transform. For the higher accuracy in the numerical integration, $\exp(-j\omega t_f)$ multiplier should be neglected, because pulse duration (t_f) is very large compared with t_r. This multiplier incorporates periodicity into the function, which renders fast numerical integration on a desktop computer impossible.

Applying vector dot product calculation mentioned in the previous section yields $G(\omega)$ expressed as

$$G(\omega) = \frac{A}{n} \cdot \frac{1 - \exp(-j\omega t_f)}{j\omega} \cdot \sum_{i=1}^{n} s_{21}^{(i)}(\omega) \exp\left(-j\omega \frac{i-1}{n} t_r\right). \tag{A11}$$

The inverse Fourier transform yields

$$g(t) = \frac{1}{2\pi} \int_{-\infty}^{\infty} G(\omega) \exp(jt\omega)\, d\omega = g_0(t) - g_0(t - t_f) \tag{A12}$$

where $g_0(t)$ is the inverse Fourier transform of $G_0(\omega)$ which is given by

$$G_0(\omega) = \frac{A}{n} \cdot \frac{1}{j\omega} \sum_{i=1}^{n} s_{21}^{(i)}(\omega) \exp\left(-j\omega \frac{i-1}{n} t_r\right). \tag{A13}$$

$g_0(t)$ is easily calculated by numerical method with much better accuracy than $g(t)$. To obtain $g_0(t)$, the following treatment was adopted.

Let $G_0(\omega)$ be

$$G_0(\omega) = X_0(\omega) - jY_0(\omega) \tag{A14}$$

where $X_0(\omega)$ and $Y_0(\omega)$ are real. The following symmetry relations exist:

$$X_0(\omega) = X_0(-\omega) \tag{A15}$$

$$Y_0(\omega) = -Y_0(-\omega). \tag{A16}$$

Using this expression, $g_0(t)$ yields

$$g_0(t) = \frac{1}{2\pi} \int_{-\infty}^{\infty} G_0(\omega) \exp(jt\omega)\, d\omega = \frac{1}{\pi} \int_0^{\infty} \{X_0(\omega) \cos(\omega t) + Y_0(\omega) \sin(\omega t)\}\, d\omega. \tag{A17}$$

Here $X_0(\omega)$ and $Y_0(\omega)$ are given by

$$X_0(\omega) = -\frac{A}{n} \sum_{i=1}^{n} \left\{ \frac{Q^{(i)}(\omega)}{\omega} \cos\left(\omega \frac{i-1}{n} t_r\right) + \frac{P^{(i)}(\omega)}{\omega} \sin\left(\omega \frac{i-1}{n} t_r\right) \right\} \tag{A18}$$

$$Y_0(\omega) = \frac{A}{n} \sum_{i=1}^{n} \left\{ \frac{P^{(i)}(\omega)}{\omega} \cos\left(\omega \frac{i-1}{n} t_r\right) - \frac{Q^{(i)}(\omega)}{\omega} \sin\left(\omega \frac{i-1}{n} t_r\right) \right\} \tag{A19}$$

where

$$s_{21}^{(i)}(\omega) = P^{(i)}(\omega) - jQ^{(i)}(\omega). \tag{A20}$$

Here $P^{(i)}(\omega)$ and $Q^{(i)}(\omega)$ are real.

In the numerical calculation of (A17), $s_{21}^{(i)}(\omega)$ is available for only a finite-frequency bandwidth, which is from 1 to 1300 MHz in the major example (8-ns input t_r), $g_0(t)$ is calculated as the following:

$$g_0(t) = \frac{1}{\pi} \int_{f=1\,\text{MHz}}^{f=1300\,\text{MHz}} \{X_0(\omega) \cos(\omega t) + Y_0(\omega) \sin(\omega t)\}\, d\omega. \tag{A21}$$

This approximation is adequate to simulate the time domain of this example, because 1-1300-MHz frequency range corresponds to 0.27-350-ns time range [6].

Acknowledgment

The authors would like to thank the various people and companies that contributed to this research with their support. I. Getreu, E. Khalily, T. Walker and R. Lefferts made significant contributions in providing assistance in the measurement facets of this work. The authors also wish to thank K. Kamei for the preparation of GaAs FET's. Hewlett-Packard, Toshiba, and Tektronix are to be thanked for invaluable logistical and technical support.

References

[1] E. Khalily, "TECAP an automated characterization system," Stanford Electronics Lab. Tech. Rep. 5017-1, Mar. 1979.

[2] "TECAP users manual," Hewlett-Packard Design Aids Tech. Rep.

DA350.4A, May 1981.
[3] "TECAP systems manual," Hewlett-Packard Design Aids Tech. Rep. DA350.4A, May 1981.
[4] "TDR difference testing with Tektronix signal processing systems," Tektronix Signal Processing Systems Application Note 4711.1, 1976.
[5] "Time domain reflectometry," Hewlett-Packard Co. Application Note 62.
[6] A. S. Farber and C. W. Ho, "Wide-band network characterization by Fourier transformation of time-domain measurements," *IEEE J. Solid-State Circuits*, vol. SC-4, no. 4, pp. 231-235.
[7] M. Ino and M. Ohmori, "Intrinsic response time of normally off MESFET's of GaAs, Si, and InP," *IEEE Trans. Microwave Theory Tech.*, vol. MTT-28, no. 5, p. 456, May 1980.
[8] J. Faricelli, J. Nulman, P. Krusius, and J. Frey, "Large signal switching response of submicron Si and GaAs MESFET's: Device vs circuit," in *Proc. 39th Annu. Device Res. Conf.*, p. IIB-8, June 1981.

First-Order Modeling of Oxide-Isolated ISL

JAN LOHSTROH, MEMBER, IEEE, AND RENÉ M. PLUTA

***Abstract*—A model is derived for an oxide-isolated ISL gate with 3-μm minimum details and fan-out = 4. The model includes an n-p-n transistor, a p-n-p transistor, a silicon diode, and four Schottky-barrier diodes. Special attention is paid to all temperature coefficients of the device parameters. Very good agreement is obtained with measurements in the temperature range from 25 to 125°C. Due to the p^+ channel-stopper in the process, the collector series resistance of the clamp p-n-p is relatively small.**

I. INTRODUCTION

AFTER the first ISL generation which was made in p-n-isolated processes [1], the second ISL generation uses oxide-isolated processes to obtain a much better performance and packing density, making it suitable for high-speed VLSI [2]-[5] and VHSIC [6].

The average propagation delay time of ISL is calculated relatively easily for low and intermediate current levels [7]; at high current levels, series resistances start to play a dominant role, which makes an analytical calculation practically impossible, so for that current region only measurements and/or computer simulations can be done [7]. For this last approach, an appropriate model which models at least all first-order effects is needed. A first-order model of p-n-isolated ISL has already been published [8].

Manuscript received July 10, 1981; revised November 27, 1981.

J. Lohstroh is with Philips Research Laboratories, Eindhoven, The Netherlands.
R. M. Pluta was with Philips Research Laboratories, Eindhoven, The Netherlands. He is now at the European Organization for Nuclear Research (CERN), Geneva, Switzerland.

In this paper, a model is derived for the oxide-isolated case, including walled emitters, buried layers (covered with oxide or epitaxial material), channel-stop ion implants, etc. Special attention is paid to temperature coefficients of resistors, capacitors, bandgap voltages, and Schottky-barrier heights. Only oxide-isolated ISL with a vertical p-n-p clamp [4] is modeled.

II. DEVICE STRUCTURE

Fig. 1 shows a top view and the cross section of an oxide-isolated ISL 3-μm minimum-detail test gate which has an additional collector contact compared with the gates used in an 21-stage ring oscillator [4] (see Fig. 2). This collector contact is used to determine some device parameters (Schottky-diode series resistance, p-n-p effective current gain, etc.); the collector contact is not used in the eventual ISL gate model, because in ISL circuits this contact is not used.

Fig. 1 shows the lateral dimensions after all the processing steps. The substrate is 5 Ω · cm and an Sb buried layer is made before epitaxial growth. The resistivity of the epitaxial layer is 0.3 Ω · cm (2×10^{16} cm^{-3}); after all the oxidation steps, the epi-thickness is reduced from 1.2 to 1.0 μm. The up-diffusion of the buried layer is 0.3 μm. Under the isolation oxide, a p-type channel stop is made to prevent n-MOS channels between the buried layers. Base and emitter junction depths are 0.5 and 0.25 μm, respectively. Fig. 3 shows the profiles. All contacts are covered with PtNi (60 percent, 40 percent) to form PtNi silicide.

Typical sheet resistances are 30 and 50 Ω/□ for the buried layer when covered with epitaxial material or oxide, respec-

0018-9383/82/0400-0675$00.75 © 1982 IEEE